The optimal P3M algorithm for computing electrostatic energies in periodic systems

V. Ballenegger[a)]
Institut UTINAM, Université de Franche-Comté, UMR 6213, 16, route de Gray, 25030 Besançon cedex, France

J. J. Cerda and O. Lenz
Frankfurt Institute for Advanced Studies, J.W. Goethe-Universität, Frankfurt, Germany

Ch. Holm
Frankfurt Institute for Advanced Studies, J.W. Goethe-Universität, Frankfurt, Germany and Max-Planck-Institut für Polymerforschung, Mainz, Germany

(Received 30 July 2007; accepted 1 November 2007; published online 16 January 2008)

We optimize Hockney and Eastwood's particle-particle particle-mesh algorithm to achieve maximal accuracy in the electrostatic energies (instead of forces) in three-dimensional periodic charged systems. To this end we construct an optimal influence function that minimizes the root-mean-square (rms) errors of the energies. As a by-product we derive a new real-space cutoff correction term, give a transparent derivation of the systematic errors in terms of Madelung energies, and provide an accurate analytical estimate for the rms error of the energies. This error estimate is a useful indicator of the accuracy of the computed energies and allows an easy and precise determination of the optimal values of the various parameters in the algorithm (Ewald splitting parameter, mesh size, and charge assignment order). © *2008 American Institute of Physics*. [DOI: 10.1063/1.2816570]

I. INTRODUCTION

Long- range interactions are ubiquitously present in our daily life. The calculation of these interactions is, however, not an easy task to perform. One needs indeed to resort to specialized algorithms to overcome the quadratic scaling with the number of particles, as soon as the simulated system includes more than a few hundred particles, see, for example, the reviews of Sagui and Darden[1] or Arnold and Holm.[2] In Molecular Dynamics (MD) simulations, one is mainly interested in the accuracy of the force computation, since they govern the dynamics of the system. In contrast, in Monte Carlo (MC) simulations, the concern is to compute accurate energies. If the potential is of long range (e.g., a Coulomb potential or dipolar interaction), and one has chosen to use periodic boundary conditions, the computation of both observables is quite time consuming if one uses the traditional Ewald sum. Since the seminal work of Hockney and co-workers[3] and Hockney and Eastwood,[4] it has been common to resort to a faster way of calculating the reciprocal space sum in the Ewald method with the help of fast Fourier transforms (FFTs), that yield a $N \log N$ scaling, where N denotes the number of charged particles. These algorithms are nowadays routinely used in MD simulations of biosystems, charged soft matter, plasmas, and many more areas.

Several variants of such mesh-based Ewald sums have been presented: the original particle-particle particle-mesh (P3M) method of Hockney and Eastwood,[5] the particle-mesh Ewald (PME) method,[6] and the smooth particle-mesh Ewald (SPME) method.[7] Comparisons of the methods have been made by Darden *et al.*,[8] Deserno and Holm,[9] and Sagui and Darden.[1] The P3M method is based on the central idea of adjusting the lattice Green function such that the mesh calculation gives on average results that are as close as possible, in a least square sense, to the exact results of the original continuum problem. In our view, this optimization of the lattice Green function distinguishes P3M from the other particle-mesh approaches. Note, however, that the mean square minimization of errors can also be implemented in a SPME approach, as has been shown for a force-interpolated SPME method.[8] This closes the historical circle, as the result is equivalent to using a lattice Green function almost indistinguishable from the original P3M one.[10]

While in the standard P3M algorithm,[4] the lattice Green function, called the "influence function," is optimized to give the best possible accuracy in the forces, the electrostatic energy is usually calculated with the same force-optimized influence function. However, there are certainly situations where one needs a high precision of the energies, for instance in Monte Carlo simulations, and the natural question arises whether one can optimize the influence function to enhance the accuracy of the P3M energies. The main goal of this paper is to derive the energy-optimized influence function, and to derive an analytical estimate for the error in the P3M energies. This error estimate is a valuable indicator of the accuracy of the calculations and allows a straightforward and precise determination of the optimal values of the various parameters in the algorithm (Ewald splitting parameter, mesh size, and charge assignment order).

The present derivation of the optimal influence function,

[a)]Electronic mail: vincent.ballenegger@univ-fcomte.fr.

 © 2008 American Institute of Physics

Author complimentary copy. Redistribution subject to AIP license or copyright, see http://jcp.aip.org/jcp/copyright.jsp

and the associated error estimate, is concise and entirely self-contained. The present paper can thus also serve as a pedagogical introduction to the main ideas and mathematics of the P3M algorithm.

The paper is organized as follows. In Sec. II, we briefly review the ideas of the standard Ewald method and provide the most important formulae. In Sec. III, we derive direct and reciprocal space correction terms which compensate, on average, the effects of cutoff errors in the standard Ewald method. We interpret the formulae in terms of the direct and reciprocal space components of the Madelung energies of the ions. In Sec. IV, the calculation of the reciprocal energy according to the P3M algorithm (i.e., with a fast Fourier transform and an optimized influence function) is presented. The mathematical analysis of the errors introduced by the discretization on a grid is performed in Sec. V. This analysis is used in Sec. VI to derive the energy-optimized influence function and the associated root-mean-square (rms) error estimate. The derivation shows that the P3M energies must be shifted to compensate for systematic cutoff and aliasing errors in the Madelung energies of the ions. Finally, our analytical results are tested numerically in Sec. VII.

II. THE EWALD SUM

We consider a system of N particles with charges q_i at positions $\boldsymbol{r}_i$ in an overall neutral and (for simplicity) cubic simulation box of length L and volume $V=L^3$. If periodic boundary conditions are applied, the total electrostatic energy of the box is given by

$$E=\frac{1}{2}\sum_{\boldsymbol{n}\in\mathbb{Z}^3}{\sum_{i,j=1}^{N}}'q_iq_jv(\boldsymbol{r}_{ij}+\boldsymbol{n}L), \tag{2.1}$$

where $v(\boldsymbol{r})=1/|\boldsymbol{r}|$ is the Coulomb potential, $\boldsymbol{r}_{ij}=\boldsymbol{r}_i-\boldsymbol{r}_j$, and $\boldsymbol{n}$ is a vector with integer components that indexes the periodic images. The prime indicates that the (divergent) summand for $i=j$ has to be omitted when $\boldsymbol{n}=0$.

Because of the slow decay of the Coulomb interaction, the sum in Eq. (2.1) is only conditionally convergent: its value is not well defined unless one specifies the precise way in which the cluster of simulation boxes is supposed to fill $\mathbb{R}^3$. Often, one chooses a spherical order of summation, which is equivalent to the limit of a large, spherically bounded, regular grid of replicas of the simulation box, embedded in vacuum. The simulation box can then be pictured as the central LEGO brick in a huge ball made up of such bricks. If this "lego ball" is surrounded by a homogeneous medium with dielectric constant ϵ' ($\epsilon'=1$ if it's vacuum) and if the simulation box has a net dipole moment $M=\Sigma_i q_i\boldsymbol{r}_i$, the particles in the ball will feel a depolarizing field created by charges that appear on the surface of the uniformly polarized ball. It can be shown that the work done against this depolarizing field when charging up the system is

$$E^{(d)}=\frac{2\pi M^2}{(1+2\epsilon')L^3} \tag{2.2}$$

in the case of a spherical order of summation[11,12] (for other summation orders, see the articles of Smith[13] and Ballenegger and Hansen[14]). The energy $E^{(d)}$ is contained, even if not easily seen, in the total electrostatic energy (2.1) [at least when $\epsilon'=1$ since such a vacuum boundary condition was assumed in writing (2.1)]. Obviously, the energy $E^{(d)}$ vanishes if we employ metallic boundary conditions defined by $\epsilon'=\infty$.

The fact that $E^{(d)}$ depends on the order of summation and, hence, on the shape of the macroscopic sample under consideration, is a consequence of the conditional convergence of the sum (2.1). Due to the energy cost $E^{(d)}$, the fluctuations of the total dipole moment of the simulation box (and, hence, of the considered macroscopic sample) depend on the dielectric constant ϵ' and on the shape of the sample. The energy $E^{(d)}$ is crucial to ensure, for example, that the dielectric constant ϵ' of the simulated system obtained from the Kirkwood formula,[15] which relates ϵ to the fluctuations of the total dipole moment, is independent of the choices made for the sample shape and for the dielectric boundary condition.[16,17]

Ewald's method to compute the energy (2.1) is based on a decomposition of the Coulomb potential, $v(\boldsymbol{r})=\psi(\boldsymbol{r})+\phi(\boldsymbol{r})$, such that $\psi(\boldsymbol{r})$ contains the short-distance behavior of the interaction, while $\phi(\boldsymbol{r})$ contains the long-distance part of the interaction and is regular at the origin. The traditional way to perform this splitting is to define

$$\phi(\boldsymbol{r})=\mathrm{erf}(\alpha r)/r,\quad r=|\boldsymbol{r}|, \tag{2.3}$$

and

$$\psi(\boldsymbol{r})=v(\boldsymbol{r})-\phi(\boldsymbol{r})=\mathrm{erfc}(\alpha r)/r. \tag{2.4}$$

With this choice, $\psi(r)$ corresponds to the interaction energy between a unit charge at a distance r from another unit charge that is screened by a neutralizing Gaussian charge distribution whose width is controlled by the Ewald length α^{-1}. Following this decomposition of the potential, the electrostatic energy can be written in the well-known Ewald form[11,18]

$$E=E^{(r)}+E^{(k)}+E^{(d)}, \tag{2.5}$$

where the real-space energy $E^{(r)}$ contains the contributions from short-range interactions $\psi(\boldsymbol{r})$, i.e.,

$$E^{(r)}=\frac{1}{2}\sum_{\boldsymbol{n}\in\mathbb{Z}^3}{\sum_{i,j=1}^{N}}'q_iq_j\psi(\boldsymbol{r}_{ij}+\boldsymbol{n}L), \tag{2.6}$$

and the reciprocal space energy $E^{(k)}$ contains contributions from long-range interactions $\phi(\boldsymbol{r})$ [apart from the contributions that are responsible for the conditional convergence which are included in the term $E^{(d)}$ in Eq. (2.5)]. The fact that the surface term (or "dipole term") $E^{(d)}$ is independent of the Ewald parameter α shows that this contribution is not specific to the Ewald method, but more generally reflects the problems inherent to the conditional convergence of the $\boldsymbol{n}$ sum in Eq. (2.1). Contrary to $E^{(r)}$ which can be computed easily in real space thanks to the rapid decay of the ψ interaction, $E^{(k)}$ is best computed in Fourier space, where it can be expressed as[18]

Author complimentary copy. Redistribution subject to AIP license or copyright, see http://jcp.aip.org/jcp/copyright.jsp

$$E^{(k)} = E^{(ks)} - E^{(s)}, \tag{2.7}$$

where

$$E^{(ks)} = \frac{1}{2L^3} \sum_{\substack{\boldsymbol{k} \in \mathbb{K} \\ \boldsymbol{k} \neq 0}} |\tilde{\rho}(\boldsymbol{k})|^2 \tilde{\phi}(\boldsymbol{k}), \tag{2.8}$$

$$E^{(s)} = Q^2 \frac{\alpha}{\sqrt{\pi}}, \tag{2.9}$$

with

$$Q^2 = \sum_{i=1}^{N} q_i^2. \tag{2.10}$$

In Eq. (2.8), $\tilde{\phi}(\boldsymbol{k})$ is the Fourier transform of the reciprocal interaction (2.3),

$$\tilde{\phi}(\boldsymbol{k}) = \int e^{-i\boldsymbol{k}\cdot\boldsymbol{r}} \phi(\boldsymbol{r}) \mathrm{d}\boldsymbol{r} = \frac{4\pi}{k^2} \exp(-k^2/4\alpha^2), \tag{2.11}$$

and $\tilde{\rho}(\boldsymbol{k})$ is the Fourier transformed charge density,

$$\tilde{\rho}(\boldsymbol{k}) = \sum_{i=1}^{N} q_i e^{-i\boldsymbol{k}\cdot\boldsymbol{r}_i}. \tag{2.12}$$

The sum in Eq. (2.8) is over wave vectors in the discrete set $\mathbb{K} = \{2\pi \boldsymbol{n}/L : \boldsymbol{n} \in \mathbb{Z}^3\}$. The term $\boldsymbol{k}=0$ is excluded in the sum because of the overall charge neutrality. The self-energy term $E^{(s)}$ compensates for the self-energies (the reciprocal interaction of each particle with itself $\frac{1}{2} q_i^2 \phi(\boldsymbol{r}=0) = q_i^2 \alpha/\sqrt{\pi}$) that are included in $E^{(ks)}$.

The energy (2.1) converges only for systems that are globally neutral. For systems with a net charge, the sum can be made convergent by adding a homogeneously distributed background charge which restores neutrality. In that case, an additional contribution[19]

$$E^{(n)} = -\frac{\pi}{2\alpha^2 L^3} \left(\sum_{i=1}^{N} q_i \right)^2 \tag{2.13}$$

must be added to Eq. (2.5) to account for the interaction energies of the charges with the neutralizing background.

The reciprocal energy $E^{(ks)}$, defined by the Ewald formula (2.7), is the starting point of mesh-based Ewald sums, which are methods to compute efficiently that energy in many-particle systems. Notice that Eq. (2.7) can also be written in an alternative form in terms of a pair potential and a Madelung self-energy, see Appendix A. The inverse length α tunes the relative weight of the real space $E^{(r)}$ and the reciprocal space $E^{(k)}$ contributions to the energy, but the final result is independent of α. In practice, $E^{(r)}$ and $E^{(k)}$ can be computed using cutoffs because the sum over $\boldsymbol{n}$ in Eq. (2.6) and the sum over $\boldsymbol{k}$ in Eq. (2.8) converge exponentially fast. Typically, one chooses α large enough to employ the minimum image convention[20] in Eq. (2.6).

At given real and reciprocal space cutoffs r_{cut} and k_{cut}, there exists actually an optimal α such that the accuracy of the approximated Ewald sum is as high as possible. This optimal value can be determined with the help of the estimates for the cutoff errors derived by Kolafa and Perram,[21] by demanding that the real and reciprocal space contributions to the error are equal. Kolafa and Perram's root-mean-square error estimates are

$$\Delta E^{(r)} \simeq Q^2 \sqrt{\frac{r_c}{2L^3}} \frac{e^{-\alpha^2 r_{\mathrm{cut}}^2}}{(\alpha r_{\mathrm{cut}})^2} \tag{2.14}$$

and

$$\Delta E^{(k)} \simeq Q^2 \alpha \frac{e^{-(k_{\mathrm{cut}}/2\alpha)^2} \sqrt{\pi}}{(k_{\mathrm{cut}} L/2)^{3/2}}. \tag{2.15}$$

These error estimates make explicit the exponential dependence of the error on the real and reciprocal space cutoffs.

Formula (2.15) is actually valid only when a correction term [given by Eq. (3.8) later] is added, to compensate the systematic error that affects the reciprocal energies when the sum over wave vectors in Eq. (2.8) is truncated. The origin of this correction term is explained in detail in Sec. III. A similar term must also be introduced in the P3M algorithm when one computes the electrostatic energy. Similarly, the direct-space energy (2.6) also contains a systematic error when the pair-wise interaction is truncated at the cutoff distance r_{cut}. The derivation in the next section will also provide a correction term for this effect.

To summarize, the final Ewald formula for the total electrostatic energy reads

$$\begin{aligned} E = {} & E^{(r)} \ [\text{Eq. (2.6)}] \\ & + E^{(ks)} \ [\text{Eq. (2.8)}] \\ & - E^{(s)} \ [\text{Eq. (2.9)}] \\ & + E^{(d)} \ [\text{Eq. (2.2)}] \\ & + E^{(n)} \ [\text{Eq. (2.13)}]. \end{aligned} \tag{2.16}$$

Furthermore, when the sums in $E^{(r)}$ and $E^{(ks)}$ are evaluated numerically using cutoffs, an additional correction term E_{cut}, defined in Eq. (3.13) later, must be added to the truncated energy, as shown in the next section.

III. CORRECTION TERM FOR TRUNCATED EWALD SUMS

If we consider electroneutral systems where the charged particles are located at random, we expect the electrostatic energy to vanish on average because there is an equal probability to find a positive or negative charge at any relative distance r. However, when periodic boundary conditions (PBC) are applied, the average energy of random systems does not vanish because each charge interacts with its own periodic images (and with the uniform neutralizing background provided by the other charges).

Since this interaction energy E_{img} of an ion with its periodic images and with the neutralizing background does not depend on the position of the ion in the simulation box, it plays the role of a "self-energy." We will refer to E_{img} as the Madelung (self-) energy of an ion, to avoid confusion with the self-energy $\frac{1}{2} q^2 \phi(0)$ already defined in the Ewald method as the reciprocal interaction of a particle with itself.

Author complimentary copy. Redistribution subject to AIP license or copyright, see http://jcp.aip.org/jcp/copyright.jsp

We denote by angular brackets the average over the positions of the N charged particles

$$\langle \cdots \rangle = \frac{1}{V^N} \int_{V^N} \cdots \mathrm{d}\boldsymbol{r}_1 \ldots \mathrm{d}\boldsymbol{r}_N. \tag{3.1}$$

A. Madelung energy

The Madelung energy of an ion takes the form $E_{\mathrm{img}} = \frac{1}{2} q^2 \zeta$, where ζ is a purely numerical factor in units of $1/L$ that depends only on the size and shape of the simulation box.

Let us calculate the average electrostatic energy of random charged systems in PBC, to find the value of ζ and derive a correction term for cutoff errors in truncated Ewald sums (some results derived here will be used in Sec. VI A). On the one hand, the average Coulomb energy of the random systems is by definition $Q^2\zeta/2$, while on the other hand, it can be calculated as the sum of a direct space contribution $\langle E^{(r)} \rangle$ and a reciprocal space contribution $\langle E^{(k)} \rangle$. The average reciprocal energy is, using Eqs. (2.8) and (2.9),

$$\langle E^{(k)} \rangle = \frac{1}{2L^3} \sum_{i,j} q_i q_j \sum_{\substack{\boldsymbol{k} \in \mathbb{K} \\ \boldsymbol{k} \neq 0}} \langle e^{-i\boldsymbol{k}\cdot(\boldsymbol{r}_i - \boldsymbol{r}_j)} \rangle \tilde{\phi}(\boldsymbol{k}) - Q^2 \frac{\alpha}{\sqrt{\pi}}. \tag{3.2}$$

Since $\langle \exp(-i\boldsymbol{k}\cdot\boldsymbol{r}_j) \rangle = \delta_{\boldsymbol{k},0}$, all terms with $j \neq i$ vanish (this is due to the fact that the Ewald pair potential averages to zero, see Appendix A). By contrast, "self" terms ($i=j$) remain and lead to

$$\langle E^{(k)} \rangle = \frac{Q^2}{2} \left(\frac{1}{L^3} \sum_{\substack{\boldsymbol{k} \in \mathbb{K} \\ \boldsymbol{k} \neq 0}} \tilde{\phi}(\boldsymbol{k}) - \frac{2\alpha}{\sqrt{\pi}} \right) = \frac{Q^2}{2} \zeta^{(k)}, \tag{3.3}$$

where the second equality defines $\zeta^{(k)}$. The average real-space energy of a single ion of charge q_i in periodic random systems is

$$\langle E_i^{(r)} \rangle = \frac{q_i^2}{2} \left(\sum_{\substack{\boldsymbol{n} \in \mathbb{Z}^3 \\ \boldsymbol{n} \neq 0}} \psi(\boldsymbol{n}L) - \frac{1}{L^3} \int_{\mathbb{R}^3} \psi(\boldsymbol{r}) \mathrm{d}^3\boldsymbol{r} \right), \tag{3.4}$$

where the first term is the sum of the direct interactions of the ion with all its periodic images, while the second term corresponds to its interaction with the uniform background charge density $-q_i/L^3$ provided by the other particles in the system. Since

$$\int_{\mathbb{R}^3} \psi(\boldsymbol{r}) \mathrm{d}^3\boldsymbol{r} = 4\pi \int_0^\infty r^2 \psi(\alpha r) \mathrm{d}r = \frac{\pi}{\alpha^2}, \tag{3.5}$$

we can write the average total real-space energy as

$$\langle E^{(r)} \rangle = \frac{Q^2}{2} \left(\sum_{\substack{\boldsymbol{n} \in \mathbb{Z}^3 \\ \boldsymbol{n} \neq 0}} \psi(\boldsymbol{n}L) - \frac{\pi}{\alpha^2 L^3} \right) = \frac{Q^2}{2} \zeta^{(r)}, \tag{3.6}$$

which defines $\zeta^{(r)}$. The second term in $\zeta^{(r)}$ takes, not surprisingly, the same form as the energy $E^{(n)}$ defined in Eq. (2.13). Notice that the earlier result for $\langle E^{(r)} \rangle$ may also be obtained by splitting Eq. (2.6) into self ($i=j$) and interaction terms, and using for the latter $\Sigma_{j \neq i} q_j = -q_i$ which follows from the electroneutrality condition. The expression of the factor $\zeta = \zeta^{(r)} + \zeta^{(k)}$ is therefore

$$\zeta = \left(\sum_{\substack{\boldsymbol{n} \in \mathbb{Z}^3 \\ \boldsymbol{n} \neq 0}} \psi(\boldsymbol{n}L) - \frac{\pi}{\alpha^2 L^3} \right) + \left(\frac{1}{L^3} \sum_{\substack{\boldsymbol{k} \in \mathbb{K} \\ \boldsymbol{k} \neq 0}} \tilde{\phi}(\boldsymbol{k}) - \frac{2\alpha}{\sqrt{\pi}} \right). \tag{3.7}$$

Equation (3.7) can be computed for a number of different box geometries.[22] For a cubic simulation box of size L, it yields[23,24]

$$\zeta \simeq -2.837297479480619610825442578061/L.$$

The earlier calculation shows that, when a charged system is simulated using PBC, the electrostatic energy (2.1) includes the contribution $Q^2\zeta/2$. The existence of this Madelung self-energy can be made more apparent in the Ewald formula for E, as shown in Appendix A.

B. Madelung cutoff error correction terms

The Ewald sums (2.6) and (2.8) are necessarily truncated when evaluated in a simulation. These truncations introduce systematic cutoff errors in the total energy because the Madelung self-energies of the ions are then not fully accounted for. This systematic error is typically of the same order of magnitude, or even larger, than the fluctuating error, due to the use of cutoffs, in the Ewald pair interaction energy.[21,25] Note that no similar systematic error affects the electrostatic forces because the Madelung energy does not depend on the position of the ion.

Fortunately, it is easy to suppress the systematic bias in the computed energies. We simply have to add the cutoff correction

$$E_{\mathrm{cut}}^{(k)} = \frac{Q^2}{2L^3} \sum_{\substack{\boldsymbol{k} \in \mathbb{K} \\ k > k_{\mathrm{cut}}}} \tilde{\phi}(\boldsymbol{k}) \tag{3.8}$$

to the computed k-space energies, which Kolafa and Perram termed the diagonal correction.[21] The value of $E_{\mathrm{cut}}^{(k)}$ does not depend on the configuration and may thus be computed in advance using a sufficiently large second cutoff $k'_{\mathrm{cut}} > k > k_{\mathrm{cut}}$. Using the definition (3.3) of $\zeta^{(k)}$, we can rewrite Eq. (3.8) as

$$E_{\mathrm{cut}}^{(k)} = \frac{Q^2}{2} (\zeta^{(k)} - \zeta_{\mathrm{cut}}^{(k)}), \tag{3.9}$$

where

$$\zeta_{\mathrm{cut}}^{(k)} = \frac{1}{L^3} \sum_{\substack{\boldsymbol{k} \in \mathbb{K} \\ \boldsymbol{k} \neq 0,\ k < k_{\mathrm{cut}}}} \tilde{\phi}(\boldsymbol{k}) - \frac{2\alpha}{\sqrt{\pi}}. \tag{3.10}$$

Similarly, if the real-space energies are computed using a cutoff $r_{\mathrm{cut}} < L/2$ (minimum image convention), we see from Eqs. (3.4)–(3.6), that the r-space cutoff correction

$$E_{\mathrm{cut}}^{(r)} = \frac{Q^2}{2} (\zeta^{(r)} - \zeta_{\mathrm{cut}}^{(r)}), \tag{3.11}$$

where

Author complimentary copy. Redistribution subject to AIP license or copyright, see http://jcp.aip.org/jcp/copyright.jsp

$$\zeta_{\mathrm{cut}}^{(r)} = -\frac{4\pi}{L^3}\int_0^{r_{\mathrm{cut}}} r^2\psi(r)\mathrm{d}r$$
$$= -\frac{2\pi}{L^3}\left(r_{\mathrm{cut}}^2 - \frac{r_{\mathrm{cut}}}{\alpha\sqrt{\pi}}e^{-\alpha^2 r_{\mathrm{cut}}^2} - \mathrm{erf}(\alpha r_{\mathrm{cut}})\left(r_{\mathrm{cut}}^2 - \frac{1}{2\alpha^2}\right)\right) \tag{3.12}$$

must be applied to the direct space energies. It is natural that the correction terms $E_{\mathrm{cut}}^{(k)}$ and $E_{\mathrm{cut}}^{(r)}$ are made up of the exact Madelung energies, minus the average Madelung energies of the ions as obtained from a calculation with direct and reciprocal space cutoffs r_{cut} and k_{cut}.

Adding Eq. (3.9) to Eq. (3.11) and using Eq. (3.7), the two cutoff corrections can be combined into a single expression

$$E_{\mathrm{cut}} = E_{\mathrm{cut}}^{(r)} + E_{\mathrm{cut}}^{(k)} = \frac{Q^2}{2}(\zeta - \zeta_{\mathrm{cut}}^{(k)} - \zeta_{\mathrm{cut}}^{(r)}). \tag{3.13}$$

All of these terms can easily be precomputed numerically before the start of a simulation.

Correcting the systematic cutoff errors in the energies with the term E_{cut} does improve significantly the accuracy of the results, especially when working with small cutoffs. In numerical tests, however, the direct space cutoff correction $E_{\mathrm{cut}}^{(r)}$ has been found to be mostly negligible compared to the reciprocal space correction $E_{\mathrm{cut}}^{(k)}$ for all practical purposes.

IV. MESH-BASED EWALD SUM

The idea of particle-mesh algorithms is to speed up the calculation of the reciprocal energy $E^{(ks)}$ with the help of a FFT. To use a fast Fourier transform, the charge density must be assigned to points on a regular grid. There are several ways to discretize the original continuum problem onto a grid.[1] We use here the P3M approach of Hockney and Eastwood,[4] as the optimization of the lattice Green function will ensure the best possible accuracy for the reciprocal energy obtained from the mesh calculation.

In the original P3M method, the splitting of the Coulomb interaction into a short-ranged part and a long-ranged part was performed in a slightly different manner than in the Ewald method. When used with Gaussian screening charge distributions,[26,27] the P3M splitting is actually equivalent to the splitting used in the Ewald method, as shown by Luty *et al.*[28] Our implementation of P3M uses the standard Ewald expressions for the decomposition into real space and reciprocal space contributions, just as the (S)PME methods.

For simplicity, we assume the number of grid points M to be identical in all three directions. Let $h=L/M$ be the spacing between two adjacent grid points. We denote by $\mathbb{M}$ the set of all grid points: $\mathbb{M}=\{\boldsymbol{m}h:\boldsymbol{m}\in\mathbb{Z}^3$ and $0\leq m_{x,y,z}<M\}$.

The mesh based calculation of the reciprocal energy is made in the following steps.

A. Assign charges to grid points

The charge density $\rho_{\mathrm{M}}(\boldsymbol{r})$ at a grid point $\boldsymbol{r}$ is computed via the equation

$$\rho_{\mathrm{M}}(\boldsymbol{r}) = \int U(\boldsymbol{r}-\boldsymbol{r}')\rho(\boldsymbol{r}')\mathrm{d}\boldsymbol{r}', \quad \boldsymbol{r}\in\mathbb{M}, \tag{4.1}$$

where $U(\boldsymbol{r})=h^{-3}W(\boldsymbol{r})$ with W as the charge assignment function (the factor h^{-3} ensures merely that $\rho_{\mathrm{M}}(\boldsymbol{r})$ has the dimensions of a density). A charge assignment function is classified according to its order P, i.e., between how many grid points per coordinate direction each charge is distributed. Typically, one chooses a cardinal B spline for W, which is a piecewise polynomial function of weight one. The Fourier transform of the charge assignment function is then

$$\tilde{W}^{(P)}(\boldsymbol{k}) = h^3\left(\frac{\sin(k_x h/2)}{k_x h/2}\frac{\sin(k_y h/2)}{k_y h/2}\frac{\sin(k_z h/2)}{k_z h/2}\right)^P, \tag{4.2}$$

where $P\in\mathbb{N}^+$ is the charge assignment order (CAO).

Notice that $\rho_{\mathrm{M}}(\boldsymbol{r})=h^{-3}\Sigma_i q_i W(\boldsymbol{r}-\boldsymbol{r}_i)$, apart at the boundaries where the periodicity has to be properly taken into account.

B. Fourier transform the charge grid

Compute the finite Fourier transform of the mesh-based charge density (using the FFT algorithm)

$$\tilde{\rho}_{\mathrm{M}}(\boldsymbol{k}) = h^3\sum_{\boldsymbol{r}\in\mathbb{M}}\rho_{\mathrm{M}}(\boldsymbol{r})e^{-i\boldsymbol{k}\cdot\boldsymbol{r}} = \mathrm{FFT}\{\rho_{\mathrm{M}}\}, \quad \boldsymbol{k}\in\tilde{\mathbb{M}}. \tag{4.3}$$

Here $\boldsymbol{k}$ is a wave vector in the reciprocal mesh $\tilde{\mathbb{M}}=\{2\pi\boldsymbol{n}/L:\boldsymbol{n}\in Z^3, |n_{x,y,z}|<M/2\}$.

We stress that $\tilde{\rho}_{\mathrm{M}}(\boldsymbol{k})$ differs from $\tilde{\rho}(\boldsymbol{k})$ even for $\boldsymbol{k}\in\tilde{\mathbb{M}}$, because sampling of the charge density on a grid introduces errors (see Sec. V).

C. Solve Poisson equation (in Fourier space)

The mesh-based electrostatic potential Φ_{M} is given by the Poisson equation, which reduces to a simple multiplication in k space

$$\tilde{\Phi}_{\mathrm{M}}(\boldsymbol{k}) = \tilde{\rho}_{\mathrm{M}}(\boldsymbol{k})\tilde{\phi}(\boldsymbol{k}), \quad \boldsymbol{k}\in\tilde{\mathbb{M}}, \tag{4.4}$$

with $\tilde{\phi}(\boldsymbol{k})$ the Fourier transformed reciprocal interaction (2.11). However, instead of using $\tilde{\phi}(\boldsymbol{k})$ in the earlier equation, it is better to introduce an "influence" function $\tilde{G}(\boldsymbol{k})$. We therefore replace Eq. (4.4) by

$$\tilde{\Phi}_{\mathrm{M}}(\boldsymbol{k}) = \tilde{\rho}_{\mathrm{M}}(\boldsymbol{k})\tilde{G}(\boldsymbol{k}), \quad \boldsymbol{k}\in\tilde{\mathbb{M}}, \tag{4.5}$$

where $\tilde{G}(\boldsymbol{k})$ is determined by the condition that it leads to the smallest possible errors in the computed energies (on average for uncorrelated random charge distributions). $\tilde{G}(\boldsymbol{k})$ will be determined later [see Eq. (6.21)]; it can be computed once and for all at the beginning of a simulation since it depends only on the mesh size and the charge assignment function. $\tilde{G}(\boldsymbol{k})$ plays basically the same role as the reciprocal interaction $\tilde{\phi}(\boldsymbol{k})$, except that it is tuned to minimize a well defined error functional in $\tilde{\rho}_{\mathrm{M}}(\boldsymbol{k})$. We stress that $\tilde{G}(\boldsymbol{k})$ is defined only for $\boldsymbol{k}\in\tilde{\mathbb{M}}$ (we dropped the subscript M on the influence function to alleviate the notation). The idea of optimizing $\tilde{G}(\boldsymbol{k})$, which is a key point of the P3M algorithm, ensures that the

Author complimentary copy. Redistribution subject to AIP license or copyright, see http://jcp.aip.org/jcp/copyright.jsp

mesh-based calculation of the reciprocal energy gives the best possible results.[4]

D. Get total reciprocal electrostatic energy

Expression (2.8) is approximated on the mesh by

$$E^{(ks)}_{\mathrm{P3M}} = \frac{1}{2L^3} \sum_{\substack{\boldsymbol{k}\in\tilde{\mathbb{M}} \\ \boldsymbol{k}\neq 0}} |\tilde{\rho}_{\mathrm{M}}(\boldsymbol{k})|^2 \tilde{G}(\boldsymbol{k}). \tag{4.6}$$

The total reciprocal energy follows from subtracting the self-energies from the earlier quantity: $E^{(k)}_{\mathrm{P3M}} = E^{(ks)}_{\mathrm{P3M}} - E^{(s)}$.

E. Electrostatic energy of individual charges (optional)

If the reciprocal energy of each individual particle is needed (and not only their sum as in step D), the potential mesh must be transformed back to real space via an inverse FFT, i.e.,

$$\Phi_{\mathrm{M}}(\boldsymbol{r}_m) = \frac{1}{L^3} \sum_{\boldsymbol{k}\in\tilde{\mathbb{M}}} \tilde{\Phi}_{\mathrm{M}}(\boldsymbol{k}) e^{i\boldsymbol{k}\cdot\boldsymbol{r}_m} = \mathrm{FFT}^{-1}\{\tilde{\Phi}_{\mathrm{M}}\}. \tag{4.7}$$

The mesh-based potential is then mapped back to the particle positions, or to any other point of interest, using the same charge assignment function

$$\Phi(\boldsymbol{r}) := \sum_{\boldsymbol{r}_m\in\mathbb{M}_p} W(\boldsymbol{r}-\boldsymbol{r}_m)\Phi_{\mathrm{M}}(\boldsymbol{r}_m). \tag{4.8}$$

In this equation, $\mathbb{M}_p = \{m h : \boldsymbol{m}\in\mathbb{Z}^3\}$ is the mesh extended by periodicity to all space, and $\Phi_{\mathrm{M}}(\boldsymbol{r})$ is assumed to be periodic (with period L). The interpretation of Eq. (4.8) is the following: due to the discretization each particle is replaced by several "subparticles" which are located at the surrounding mesh points and carry the fraction $W(\boldsymbol{r}-\boldsymbol{r}_m)$ of the charge of the original particle. The potential at the position of the original particle is given by the sum of the charge fraction times the potential at each mesh points. The reciprocal electrostatic energy of the ith particle is then $q_i\Phi(\boldsymbol{r}_i)/2$, and the total reciprocal energy (including self-energies) is the sum

$$E^{(ks)}_{\mathrm{P3M}} = \frac{1}{2}\int_V \rho(\boldsymbol{r})\Phi(\boldsymbol{r})\mathrm{d}\boldsymbol{r} = \frac{1}{2}\sum_i q_i\Phi(\boldsymbol{r}_i). \tag{4.9}$$

This formula gives the same result for the total energy as Eq. (4.6). A mathematical proof of the equivalence is given in Appendix B.

V. ANALYSIS OF DISCRETIZATION ERRORS

If the fast Fourier transform has the benefit of speed, it has the drawback of introducing errors in the k-space spectrum of the charge density: $\tilde{\rho}_{\mathrm{M}}(\boldsymbol{k})$ differs from the true Fourier transform (2.12) [times a trivial factor $\tilde{U}(\boldsymbol{k})$] because of the discretization on a finite grid.

The difference is twofold. First, $\tilde{\rho}(\boldsymbol{k})$ is defined for any vector in the full k-space $\mathbb{K}$, whereas $\tilde{\rho}_{\mathrm{M}}(\boldsymbol{k})$ is defined only for $\boldsymbol{k}\in\tilde{\mathbb{M}}$, i.e., in the first Brillouin zone. This is a first natural consequence of discretization: if the grid spacing is h, it necessarily introduces a cutoff $|k_{x,y,z}| < \pi/h$ in k space. Second, the act of sampling the charge density at grid points, which is mathematically embodied in Eq. (4.3) by the presence of a discrete Fourier transform instead of a continuous FT, introduces aliasing errors. While a continuous FT would simply transform the convolution Eq. (4.1) into

$$\mathrm{FT}\{\rho_{\mathrm{M}}\}(\boldsymbol{k}) = \tilde{U}(\boldsymbol{k})\tilde{\rho}(\boldsymbol{k}), \quad \boldsymbol{k}\in\mathbb{K}, \tag{5.1}$$

the finite Fourier transform results in (see proof in Appendix C)

$$\tilde{\rho}_{\mathrm{M}}(\boldsymbol{k}) = \mathrm{FFT}\{\rho_{\mathrm{M}}\}(\boldsymbol{k}) = \sum_{\boldsymbol{m}\in\mathbb{Z}^3} \tilde{U}(\boldsymbol{k}+\boldsymbol{m}k_g)\tilde{\rho}(\boldsymbol{k}+\boldsymbol{m}k_g), \boldsymbol{k}\in\tilde{\mathbb{M}}, \tag{5.2}$$

where $k_g = 2\pi/h$. The sum over $\boldsymbol{m}$ shows that spurious contributions from high frequencies of the full spectra $\tilde{U}(\boldsymbol{k})\tilde{\rho}(\boldsymbol{k})$ are introduced into the first Brillouin zone $\tilde{\mathbb{M}}$. These unwanted copies of the other Brillouin zones into the first one are known as aliasing errors.[4]

To avoid aliasing errors, the spectrum needs to be entirely contained within the first Brillouin zone. Since $\tilde{\rho}(\boldsymbol{k})$ may contain arbitrary high frequencies, this can only be achieved by choosing $U(\boldsymbol{k})$ to be a low-pass filter satisfying $\tilde{U}(\boldsymbol{k})=0$ for $\boldsymbol{k}\in\mathbb{K}\setminus\tilde{\mathbb{M}}$. But the charge assignment function would then have a compact support in k space and, hence, an infinite support in r space. This is not acceptable, as it would require the grid to have an infinite extension. The need to keep the charge assignment function local in r space means that $\tilde{U}(\boldsymbol{k})$ cannot be a perfect low pass filter. Aliasing errors are therefore unavoidable, and the impact of these errors must be minimized, by choosing a good compromise for the charge assignment function and optimizing the influence function. The influence function can indeed compensate partially for the aliasing errors because the spectra of $\tilde{U}(\boldsymbol{k})$ and $\tilde{\phi}(\boldsymbol{k})$ are known exactly at all frequencies.

The error in reciprocal energy, for a given configuration $\rho(\boldsymbol{r})$ of the charges, is defined by the difference

$$\Delta E^{(k)} = E^{(k)}_{\mathrm{P3M}} - E^{(k)}, \tag{5.3}$$

where $E^{(k)}$ is the exact reciprocal energy [see Eqs. (2.8) and (2.9)]. The earlier analysis of discretization errors results in the explicit formula for this error

$$\Delta E^{(k)} = \frac{1}{2L^3} \sum_{\substack{\boldsymbol{k}\in\tilde{\mathbb{M}} \\ \boldsymbol{k}\neq 0}} |\tilde{\rho}_{\mathrm{M}}(\boldsymbol{k})|^2 \tilde{G}(\boldsymbol{k}) - \frac{1}{2L^3} \sum_{\substack{\boldsymbol{k}\in\mathbb{K} \\ \boldsymbol{k}\neq 0}} |\tilde{\rho}(\boldsymbol{k})|^2 \tilde{\phi}(\boldsymbol{k}), \tag{5.4}$$

where $\tilde{\rho}_{\mathrm{M}}(\boldsymbol{k})$ is given by Eq. (5.2). The error $\Delta E^{(k)}$ is due to the finite resolution h offered by the mesh. The finiteness of h introduces the cutoff π/h in k space ($\boldsymbol{k}\in\tilde{\mathbb{M}}$) and causes aliasing errors [$\tilde{\rho}_{\mathrm{M}}(\boldsymbol{k}) \neq \tilde{\rho}(\boldsymbol{k})\tilde{U}(\boldsymbol{k})$] that cannot be entirely eliminated by the charge assignment function.

Author complimentary copy. Redistribution subject to AIP license or copyright, see http://jcp.aip.org/jcp/copyright.jsp

VI. OPTIMIZATION OF THE P3M ALGORITHM

We derive in this section the influence function $\tilde{G}(\boldsymbol{k})$ that minimizes the error (5.4) on average for uncorrelated systems and we give a formula for the associated rms errors. The average over random systems is denoted by angular brackets, as in Sec. III.

Notice that the assumption of the absence of correlations is never satisfied in practice (even for uniform systems because negative charges tend to cluster around positive charges and vice-versa). The error estimate proves, however, to predict quite accurately the error in real systems with correlations, notably in liquids where the pair distribution function $g(r)$ decays rapidly to one.

A. Shift in the energies to avoid systematic errors

The P3M energies (4.6) contain in general systematic errors, i.e., $\langle \Delta E^{(k)} \rangle \neq 0$, because the Madelung energies of the ions obtained in the mesh calculation contain cut-off and aliasing errors. The average error

$$K = \langle \Delta E^{(k)} \rangle = \langle E^{(k)}_{\mathrm{P3M}} \rangle - \langle E^{(k)} \rangle \tag{6.1}$$

is a constant that must be subtracted from the P3M energies, to ensure that the energies are right on average. The corrected P3M energies are thus obtained by applying a constant shift to the original P3M energies

$$E^{(k)}_{\mathrm{P3M,corr}} = E^{(k)}_{\mathrm{P3M}} - K, \tag{6.2}$$

where the constant K depends on the various P3M parameters like mesh size, CAO, and Ewald splitting parameter.

Let us determine analytically the constant (6.1). Writing it as $K = \langle E^{(k)}_{\mathrm{P3M}} \rangle - \langle E^{(k)} \rangle$, we can use the result (3.3) for $\langle E^{(k)} \rangle$: it is nothing but $Q^2 \zeta^{(k)}/2$, i.e., the k-space Madelung energies of the ions. The other term $\langle E^{(k)}_{\mathrm{P3M}} \rangle$ can be calculated in the same way as Eq. (3.2). Using Eqs. (4.6), (5.2), and (2.9), we find

$$\langle E^{(k)}_{\mathrm{P3M}} \rangle = \frac{Q^2}{2} \left(\frac{1}{L^3} \sum_{\substack{\boldsymbol{k} \in \tilde{\mathbb{M}} \\ \boldsymbol{k} \neq 0}} \tilde{G}(\boldsymbol{k}) \sum_{\boldsymbol{m} \in \mathbb{Z}^3} \tilde{U}^2(\boldsymbol{k} + k_g \boldsymbol{m}) - \frac{2\alpha}{\sqrt{\pi}} \right)$$

$$= \frac{Q^2}{2} \zeta^{(k)}_{\mathrm{P3M}}, \tag{6.3}$$

which defines $\zeta^{(k)}_{\mathrm{P3M}}$. The result (6.3) can be interpreted as the average k-space Madelung energies of the ions as obtained from the mesh calculation, i.e., including cutoff and aliasing errors. The explicit expression of the correction constant (6.1) is thus

$$K = \frac{Q^2}{2} (\zeta^{(k)}_{\mathrm{P3M}} - \zeta^{(k)})$$

$$= \frac{Q^2}{2L^3} \left(\sum_{\substack{\boldsymbol{k} \in \tilde{\mathbb{M}} \\ \boldsymbol{k} \neq 0}} \tilde{G}(\boldsymbol{k}) \sum_{\boldsymbol{m} \in \mathbb{Z}^3} \tilde{U}^2(\boldsymbol{k} + k_g \boldsymbol{m}) - \sum_{\substack{\mathbf{k} \in K \\ \mathbf{k} \neq 0}} \tilde{\phi}(\boldsymbol{k}) \right). \tag{6.4}$$

In the last sum in (6.4), the terms with $|k_{x,y,z}| > \pi/h$ are equivalent to the k-space cutoff correction defined in Eq. (3.8). These terms compensate for the fact that the Madelung energies of the ions are underestimated in the mesh calculation because of the cutoff π/h introduced by the finite size of the mesh. The remaining terms in Eq. (6.4) compensate, on average, the aliasing errors that affect the Madelung energies of the ions obtained from the mesh calculation.

Notice that the two correction terms $E^{(r)}_{\mathrm{cut}}$ and $-K$ can be combined together in the simple expression

$$E^{\mathrm{cut}}_{\mathrm{P3M}} = E^{(r)}_{\mathrm{cut}} - K = \frac{Q^2}{2} (\zeta - \zeta^{(k)}_{\mathrm{P3M}} - \zeta^{(r)}_{\mathrm{cut}}), \tag{6.5}$$

where ζ is defined by Eq. (3.7) and $\zeta^{(r)}_{\mathrm{cut}}$ is given in Eq. (3.12). We stress that $E^{\mathrm{cut}}_{\mathrm{P3M}}$ has the same structure as the correction term (3.13) for truncated Ewald sums. The difference lies in the replacement of $\zeta^{(k)}_{\mathrm{cut}}$ by the quantity $\zeta^{(k)}_{\mathrm{P3M}}$ defined in Eq. (6.3), which accounts for both the cutoff and aliasing errors that affect the reciprocal energies computed on the mesh.

In summary, the final formula for computing the total electrostatic energy with the P3M algorithm is

$$\begin{aligned} E \approx\ & E^{(r)} \ [\text{Eq. (2.6)}] \\ & + E^{(ks)}_{\mathrm{P3M}} \ [\text{Eq. (4.6)}] \\ & - E^{(s)} \ [\text{Eq. (2.9)}] \\ & + E^{(d)} \ [\text{Eq. (2.2)}] \\ & + E^{(n)} \ [\text{Eq. (2.13)}] \\ & + E^{\mathrm{cut}}_{\mathrm{P3M}} \ [\text{Eq. (6.5)}]. \end{aligned} \tag{6.6}$$

The correction term $E^{\mathrm{cut}}_{\mathrm{P3M}}$ is necessary to compensate on average for systematic errors in the mesh calculation. It can be computed once for all before the start of a simulation, since it depends only on the size of the simulation box, the size of a mesh cell, the charge assignment function, and the influence function.

B. rms error estimate for energy

The result (5.4) is an exact measure of the error in the P3M energies for a given configuration $\rho(\boldsymbol{r})$ of the particles. Let us average this expression over all possible positions of the particles to get a useful overall measure of the accuracy of the algorithm. The rms error of the corrected P3M energies is, by definition,

$$(\Delta E^{(k)}_{\mathrm{rms}})^2 := \langle (E^{(k)}_{\mathrm{P3M,corr}} - E^{(k)})^2 \rangle = \langle (\Delta E^{(k)} - K)^2 \rangle, \tag{6.7}$$

where we used Eqs. (5.3) and (6.2). We can isolate in $\Delta E^{(k)}$ "interaction" terms $(i \neq j)$ from self-terms $(i=j)$,

$$(\Delta E^{(k)}_{\mathrm{rms}})^2 = \langle (\Delta E^{(k)}_{\mathrm{int}} + \Delta E^{(k)}_{\mathrm{self}} - K)^2 \rangle. \tag{6.8}$$

We recall from Sec. III that the interaction terms vanish on average for random systems: $\langle \Delta E^{(k)}_{\mathrm{int}} \rangle = 0$. The correlation

$$\langle \Delta E^{(k)}_{\mathrm{self}} \Delta E^{(k)}_{\mathrm{int}} \rangle = 0 \tag{6.9}$$

Author complimentary copy. Redistribution subject to AIP license or copyright, see http://jcp.aip.org/jcp/copyright.jsp

vanishes as well for the same reason (this is due to the fact that the average Ewald interaction energy between a fixed particle i and a particle $j \neq i$ is zero, see Appendix A). Equation (6.8) therefore reduces to

$$(\Delta E^{(k)}_{\mathrm{rms}})^2 = \langle (\Delta E^{(k)}_{\mathrm{int}})^2 \rangle + \langle (\Delta E^{(k)}_{\mathrm{self}} - K)^2 \rangle, \tag{6.10}$$

where the first term accounts for fluctuating errors in the interactions energies and the second term accounts for fluctuating errors in the corrected Madelung self-energies of the ions. Since the latter term may be written as

$$\langle (\Delta E^{(k)}_{\mathrm{self}} - K)^2 \rangle = \langle (\Delta E^{(k)}_{\mathrm{self}})^2 \rangle - K^2, \tag{6.11}$$

we remark that the shift $-K$ derived in the previous section, in addition to removing the systematic bias in the k-space energies, also reduces the fluctuating errors of the k-space self-energies by an amount $-K^2$.

In the subtraction $\Delta E^{(k)}_{\mathrm{self}} - K$, it can be seen, from Eq. (5.4) in which only $i=j$ terms are kept and Eq. (6.4), that all terms containing $\tilde{\phi}(\boldsymbol{k})$ cancel out, so we have

$$\langle (\Delta E^{(k)}_{\mathrm{self}} - K)^2 \rangle = \left\langle \left(\frac{1}{2L^3} \sum_{\substack{\boldsymbol{k} \in \tilde{\mathbb{M}} \\ \boldsymbol{k} \neq 0}} \tilde{G}(\boldsymbol{k}) \sum_i q_i^2 \left[\sum_{\boldsymbol{m}_1} \sum_{\boldsymbol{m}_2} \tilde{U}(\boldsymbol{k}_{\boldsymbol{m}_1}) \tilde{U}(\boldsymbol{k}_{\boldsymbol{m}_2}) e^{i k_g (\boldsymbol{m}_1 - \boldsymbol{m}_2) \cdot \boldsymbol{r}_i} - \sum_{\boldsymbol{m}} \tilde{U}^2(\boldsymbol{k}_{\boldsymbol{m}}) \right] \right)^2 \right\rangle, \tag{6.12}$$

where we used the symmetry $\tilde{U}(-\boldsymbol{k}) = \tilde{U}(\boldsymbol{k})$ and introduced the shorthand notation $\boldsymbol{k}_{\boldsymbol{m}} = \boldsymbol{k} + k_g \boldsymbol{m}$. When the square is expanded, the summation over particles Σ_i becomes a double summation $\Sigma_{i,i'}$. All terms with $i' \neq i$ vanish, because $\langle \exp(i k_g (\boldsymbol{m}_1 - \boldsymbol{m}_2) \cdot \boldsymbol{r}_i) \rangle = \delta_{\boldsymbol{m}_1, \boldsymbol{m}_2}$, leaving identical sums over $\boldsymbol{m}$ which cancel each other. The remaining terms $i' = i$ evaluate to

$$\langle (\Delta E^{(k)}_{\mathrm{self}} - K)^2 \rangle = \frac{1}{4L^6} \left(\sum_i q_i^4 \right) \sum_{\substack{\boldsymbol{k} \in \tilde{\mathbb{M}} \\ \boldsymbol{k} \neq 0}} \sum_{\substack{\boldsymbol{k}' \in \tilde{\mathbb{M}} \\ \boldsymbol{k}' \neq 0}} \tilde{G}(\boldsymbol{k}) \tilde{G}(\boldsymbol{k}') \left\{ \sum_{\boldsymbol{m}_1} \sum_{\boldsymbol{m}_2} \sum_{\boldsymbol{m}_3} \tilde{U}(\boldsymbol{k}_{\boldsymbol{m}_1}) \tilde{U}(\boldsymbol{k}_{\boldsymbol{m}_2}) \tilde{U}(\boldsymbol{k}'_{\boldsymbol{m}_3}) \tilde{U}(\boldsymbol{k}'_{\boldsymbol{m}_1 - \boldsymbol{m}_2 + \boldsymbol{m}_3}) \right.$$
$$\left. - \sum_{\boldsymbol{m}} \tilde{U}^2(\boldsymbol{k}_{\boldsymbol{m}}) \cdot \sum_{\boldsymbol{m}'} \tilde{U}^2(\boldsymbol{k}'_{\boldsymbol{m}'}) \right\} = \frac{1}{4L^3} \left(\sum_i q_i^4 \right) H^2_{\mathrm{self}} \tag{6.13}$$

with

$$H^2_{\mathrm{self}} = \frac{1}{L^3} \sum_{\substack{\boldsymbol{k} \in \tilde{\mathbb{M}} \\ \boldsymbol{k} \neq 0}} \sum_{\substack{\boldsymbol{k}' \in \tilde{\mathbb{M}} \\ \boldsymbol{k}' \neq 0}} \tilde{G}(\boldsymbol{k}) \tilde{G}(\boldsymbol{k}') \left\{ \sum_{\boldsymbol{m}_1} \sum_{\boldsymbol{m}_2 \neq \boldsymbol{m}_1} \sum_{\boldsymbol{m}_3} \tilde{U}(\boldsymbol{k}_{\boldsymbol{m}_1}) \tilde{U}(\boldsymbol{k}_{\boldsymbol{m}_2}) \tilde{U}(\boldsymbol{k}'_{\boldsymbol{m}_3}) \tilde{U}(\boldsymbol{k}'_{\boldsymbol{m}_1 - \boldsymbol{m}_2 + \boldsymbol{m}_3}) \right\}. \tag{6.14}$$

The fluctuating errors of the Madelung self-energies scale therefore like $\Sigma_i q_i^4$ with the valencies of the ions. The prefactor is somewhat complicated since it involves a double summation over wave vectors and a triple summation over alias indices $\boldsymbol{m}_1$, $\boldsymbol{m}_2$, $\boldsymbol{m}_3$, but H^2_{self} can be evaluated reasonably fast. The numerical calculation of H^2_{self} can be accelerated by taking profit of the symmetries (the sum over $\boldsymbol{k}$ can be restricted to only half an octant of the reciprocal mesh) and by skipping inner loops in the triple summation over alias indices if the product of the charge fractions is almost zero.

We calculate now the fluctuations of the errors in the interaction energies, i.e., the first term of Eq. (6.10). That term reads, using Eqs. (6.8), (5.4), (5.2), and (2.12) and keeping only interaction terms

$$\langle (\Delta E^{(k)}_{\mathrm{int}})^2 \rangle = \left\langle \left(\frac{1}{2L^3} \sum_{\substack{\boldsymbol{k} \in \tilde{\mathbb{M}} \\ \boldsymbol{k} \neq 0}} \sum_{\substack{i,j \\ i \neq j}} q_i q_j \sum_{\boldsymbol{m} \in \mathbb{Z}^3} e^{i \boldsymbol{k}_{\boldsymbol{m}} \cdot \boldsymbol{r}_i} \left[\tilde{G}(\boldsymbol{k}) \sum_{\boldsymbol{m}' \in \mathbb{Z}^3} e^{-i \boldsymbol{k}_{\boldsymbol{m}'} \cdot \boldsymbol{r}_j} \tilde{U}(\boldsymbol{k}_{\boldsymbol{m}}) \tilde{U}(\boldsymbol{k}_{\boldsymbol{m}'}) - e^{-i \boldsymbol{k}_{\boldsymbol{m}} \cdot \boldsymbol{r}_j} \tilde{\phi}(\boldsymbol{k}_{\boldsymbol{m}}) \right] \right)^2 \right\rangle. \tag{6.15}$$

The calculation of this average is straightforward, though somewhat tedious. We find that it reduces to

$$\langle (\Delta E^{(k)}_{\mathrm{int}})^2 \rangle \simeq \frac{Q^4}{4L^3} H^2_{\mathrm{int}}, \tag{6.16}$$

where

$$H^2_{\mathrm{int}} = \frac{2}{L^3} \sum_{\substack{\boldsymbol{k} \in \tilde{\mathbb{M}} \\ \boldsymbol{k} \neq 0}} \left[\tilde{G}^2(\boldsymbol{k}) \left(\sum_{\boldsymbol{m}} \tilde{U}^2(\boldsymbol{k}_{\boldsymbol{m}}) \right)^2 - 2 \tilde{G}(\boldsymbol{k}) \sum_{\boldsymbol{m}} \tilde{U}^2(\boldsymbol{k}_{\boldsymbol{m}}) \tilde{\phi}(\boldsymbol{k}_{\boldsymbol{m}}) + \sum_{\boldsymbol{m}} \tilde{\phi}^2(\boldsymbol{k}_{\boldsymbol{m}}) \right]. \tag{6.17}$$

Author complimentary copy. Redistribution subject to AIP license or copyright, see http://jcp.aip.org/jcp/copyright.jsp

The factor 2 in H_{int}^2 originates from the fact that each pair of particles appears twice in the sum over i and $j \neq i$ in Eq. (6.15). Expression (6.17) is the analog for the energy of the parameter Q introduced by Hockney and Eastwood to measure the accuracy of the P3M forces.[4] Notice that Eq. (6.17) is given in real space by

$$H_{\text{int}}^2 = \frac{2}{V_{\text{cell}}} \int_{V_{\text{cell}}} d\boldsymbol{r}_1 \int_{L^3} d\boldsymbol{r} [\phi_{\text{P3M}}(\boldsymbol{r};\boldsymbol{r}_1) - \phi(\boldsymbol{r}-\boldsymbol{r}_1)]^2, \tag{6.18}$$

where $\phi_{\text{P3M}}(\boldsymbol{r};\boldsymbol{r}_1)$ is the reciprocal potential at $\boldsymbol{r}$ created by a unit charge located at $\boldsymbol{r}_1$, as obtained from the P3M algorithm. [This potential is given in Fourier space by combining Eq. (C4) with Eq. (5.2) in which we set $\rho(\boldsymbol{r}) = \delta(\boldsymbol{r}-\boldsymbol{r}_1)$.] H_{int}^2 is, hence, twice the squared deviation between the potential ϕ_{P3M} obtained from the mesh calculation and the exact reciprocal potential ϕ, summed over all relative positions $\boldsymbol{r}$ within the simulation box, and averaged over all possible positions of charge $\boldsymbol{r}_1$ in a mesh cell ($V_{\text{cell}} = h^3$).

Inserting the earlier results in Eq. (6.10), our final expression for the rms error of the (corrected) P3M energies is

$$\Delta E_{\text{rms}}^{(k)} = \frac{\sqrt{Q^4 H_{\text{int}}^2 + (\sum_i q_i^4) H_{\text{self}}^2}}{2L^{3/2}}, \tag{6.19}$$

where H_{int}^2 and H_{self}^2 are defined in Eqs. (6.17) and (6.14). This error depends on the influence function $\tilde{G}(\boldsymbol{k})$. The optimal influence function (the one that minimizes the error) will be determined in the next section. The earlier error estimate, together with the optimal influence function (6.21) and the constant shift (6.4) which must be applied to the P3M energies, constitute the main results of this paper.

The rms error (6.19) displays two different scalings with the valences of the ions: $(\Sigma_i q_i^2)^2$ for errors coming from pair interactions (such a scaling also governs errors in P3M forces[29]) and $\Sigma_i q_i^4$ for errors in Madelung self-energies. Because of these different scalings, the errors from pair interactions are expected to dominate in systems with many charged particles ($Q^4 \gg \Sigma_i q_i^4$). Notice that H_{self}^2 is, roughly speaking, proportional to $(\Sigma_{\boldsymbol{k}} \tilde{G}(\boldsymbol{k}))^2$, while H_{self}^2 scales like $\Sigma_{\boldsymbol{k}} \tilde{G}^2(\boldsymbol{k})$. The errors in the Madelung self-energies increase therefore more rapidly than the errors in the pair interaction energies when the Ewald splitting parameter α [and, hence, $\tilde{G}(\boldsymbol{k})$] is increased, or when the size of the mesh is increased. The importance of the two source of errors (fluctuations in pair interaction energies versus fluctuations in Madelung self-energies) will be compared in Sec. VII for a test system with $Q^2 = 100$.

C. Optimal influence function

We can now determine the optimal influence function $\tilde{G}(\boldsymbol{k})$, by imposing the condition that it minimizes the rms error (6.19). Since the errors coming from pair P3M interactions are expected to dominate the self-interaction errors (except in systems with few particles), we optimize the influence function only with respect to the pair interactions. Setting

$$\frac{\delta H_{\text{int}}^2}{\delta \tilde{G}(\boldsymbol{k})} = 0, \tag{6.20}$$

gives immediately

$$\tilde{G}(\boldsymbol{k}) = \frac{\sum_{\boldsymbol{m} \in \mathbb{Z}^3} \tilde{U}^2(\boldsymbol{k}_{\boldsymbol{m}}) \tilde{\phi}(\boldsymbol{k}_{\boldsymbol{m}})}{\left(\sum_{\boldsymbol{m} \in \mathbb{Z}^3} \tilde{U}^2(\boldsymbol{k}_{\boldsymbol{m}}) \right)^2}, \tag{6.21}$$

where we recall that the Fourier-transformed reciprocal interaction $\tilde{\phi}(\boldsymbol{k})$ is given by Eq. (2.11). An optimization of the influence function with respect to the full rms error could be performed, but would require solving a linear system of M^3 equations to compute $\tilde{G}(\boldsymbol{k})$. The numerical results shown in Sec. VII will confirm that such a full optimization is not necessary in typical systems.

Since $\tilde{\phi}(\boldsymbol{k})$ decays exponentially fast, the optimal influence function is given in good approximation by

$$\tilde{G}(\boldsymbol{k}) \simeq \tilde{\phi}(\boldsymbol{k}) \frac{\tilde{U}^2(\boldsymbol{k})}{\left(\sum_{\boldsymbol{m} \in \mathbb{Z}^3} \tilde{U}^2(\boldsymbol{k}_{\boldsymbol{m}}) \right)^2}. \tag{6.22}$$

$\tilde{G}(\boldsymbol{k})$ differs thus from $\tilde{\phi}(\boldsymbol{k})$ by a factor which is always less than 1. This damping of the interaction compensates as well as possible for the aliasing errors introduced by the use of a fast Fourier transform. If $\tilde{U}(\boldsymbol{k})$ were a perfect low-pass filter [$\tilde{U}(\boldsymbol{k}_{\boldsymbol{m}}) = 0$ if $\boldsymbol{m} \neq 0$], no aliasing error would occur and the influence function would reduce to $\tilde{G}(\boldsymbol{k}) = \tilde{\phi}(\boldsymbol{k}) / \tilde{U}^2(\boldsymbol{k})$. This is indeed the result expected from Eq. (5.4) when aliasing errors are absent. The true optimal influence function (6.21) differs from this simple expression by contributions from the high-frequency spectrum of $\tilde{U}(\boldsymbol{k})$ and reciprocal interaction (2.11).

Hockney and Eastwood obtained the following optimal influence function by minimizing the errors in the forces instead of the energy[4]

$$\tilde{G}^{(\text{forces})}(\boldsymbol{k}) = \frac{\sum_{\boldsymbol{m}} (\boldsymbol{k} \cdot \boldsymbol{k}_{\boldsymbol{m}}) \tilde{U}^2(\boldsymbol{k}_{\boldsymbol{m}}) \tilde{\phi}(\boldsymbol{k}_{\boldsymbol{m}})}{\boldsymbol{k}^2 \left(\sum_{\boldsymbol{m}} \tilde{U}^2(\boldsymbol{k}_{\boldsymbol{m}}) \right)^2}. \tag{6.23}$$

Obviously, this function is also given in very good approximation by Eq. (6.22). This explains why influence functions (6.21)–(6.23) all give very similar results when computing energies and forces.

Inserting Eq. (6.21) into Eq. (6.17), we find that the minimal value of H_{int}^2 is

$$H_{\text{int}}^2|_{\text{min}} = \frac{1}{L^3} \sum_{\substack{\boldsymbol{k} \in \tilde{\mathbb{M}} \\ \boldsymbol{k} \neq 0}} \left[\sum_{\boldsymbol{m} \in \mathbb{Z}^3} \tilde{\phi}^2(\boldsymbol{k}_{\boldsymbol{m}}) - \left(\frac{\sum_{\boldsymbol{m}} \tilde{U}^2(\boldsymbol{k}_{\boldsymbol{m}}) \tilde{\phi}(\boldsymbol{k}_{\boldsymbol{m}})}{\sum_{\boldsymbol{m}} \tilde{U}^2(\boldsymbol{k}_{\boldsymbol{m}})} \right)^2 \right]. \tag{6.24}$$

This is the expression of H_{int}^2 to be used in the rms error estimate (6.19) when the P3M algorithm is optimized to

Author complimentary copy. Redistribution subject to AIP license or copyright, see http://jcp.aip.org/jcp/copyright.jsp

yield the smallest possible errors in the pair interaction energies.

We recall that the errors in the P3M energies originate from aliasing effects (due to the sampling on a grid) and truncation errors (due to the fact that the reciprocal mesh contains only a finite number of wave vectors). The truncation error can only be reduced by choosing a larger mesh or by using a reciprocal interaction with a faster decay in k space, whereas the aliasing errors may be reduced by increasing the order of the charge assignment function (up to the maximum order allowed by the size of the mesh). The intrinsic truncation error of a given mesh and reciprocal interaction can be obtained by assuming $\tilde{U}(\boldsymbol{k})$ in Eq. (6.24) to be a perfect low-pass filter

$$H^2_{\text{int,cutoff}}|_{\min} = \frac{1}{L^3} \sum_{\substack{\boldsymbol{k} \in \tilde{\mathbb{M}} \\ \boldsymbol{k} \neq 0}} \left[\sum_{\boldsymbol{m} \in \mathbb{Z}^3} \tilde{\phi}^2(\boldsymbol{k}_{\boldsymbol{m}}) - \tilde{\phi}^2(\boldsymbol{k}) \right]. \quad (6.25)$$

By inserting this formula in Eq. (6.19), we get an estimate of the intrinsic rms cutoff error in k space caused by the finite number of wave vectors in the reciprocal mesh. The rms error associated with Eq. (6.25) depends only on the size of the mesh and on the choice of the reciprocal interaction, i.e., Ewald parameter α if the standard form (2.3) is used.

VII. NUMERICAL CHECK OF ACCURACY

In this section, we test the analytical results (optimal influence function, energy shift $E^{\text{cut}}_{\text{P3M}}$, rms error estimate) derived in the previous section. We do this by comparing the P3M energies with the exact energies calculated in a specific random system. In the following, all dimensions are given in terms of the arbitrary length unit $\mathcal{L}$ and charge unit $\mathcal{C}$. In particular, energies and energy errors are given in units of $\mathcal{C}^2/\mathcal{L}$. We choose the same test system as the one defined in Appendix D of Deserno and Holm:[9] 100 particles randomly distributed within a cubic box of length $L=10\mathcal{L}$, half of them carry a positive, the other half a negative unit charge. The statistical average $\langle \cdots \rangle$ is calculated by averaging over at least 100 different configurations of this test system (these configurations are determined by using the same random number generator as in Deserno and Holm[9]). Well converged Ewald sums (in metallic boundary conditions) were used to compute the exact energies of the test systems. The first three systems have energies −15.43059, −15.26641, and −15.59147, respectively, values that are all quite close to the Madelung energies of the ions $Q^2\zeta/2 \simeq -14.187$.

The P3M energies of the test systems were computed with various mesh sizes ($M=4,8,16,32$), a real-space cutoff $r_{\text{cut}}=4.95$, and different orders of the charge assignment function (from 1 to 7). Our calculations show that using the energy-optimized influence function (6.21), instead of the force-optimized influence function (6.23), leaves the energies almost unchanged. (A slight improvement in accuracy appears only when the aliasing error are at their maximum, namely for a charge assignment order of 1 and large values of α.) This behavior could have been expected, since both influence functions are almost equivalent to the simple formula (6.22).

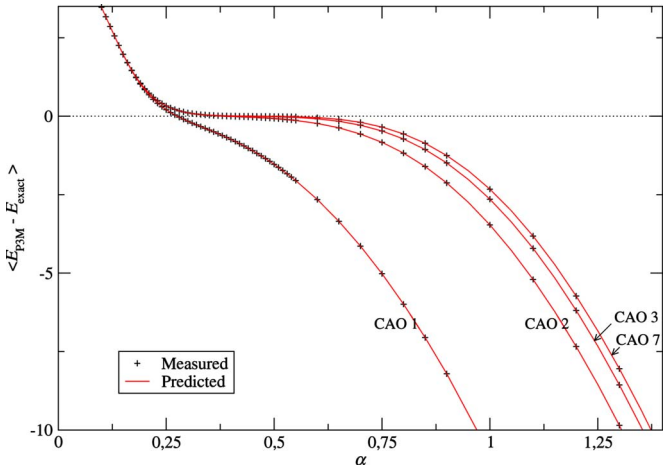

FIG. 1. (Color online) Comparison between the measured systematic error of the uncorrected P3M energies (crosses) and the theoretical prediction $-E^{\text{cut}}_{\text{P3M}}$ (solid lines) as a function of Ewald parameter α. The average is performed over 1000 test systems consisting in 100 charges located at random in a box of size $L=10$. The mesh has size $M=8$ and the real-space cutoff is $r_{\text{cut}}=4.95$.

We compare in Fig. 1 the measured systematic error $\langle E_{\text{P3M}} - E_{\text{exact}} \rangle$ of the uncorrected P3M energies [Eq. (6.6) without term $E^{\text{cut}}_{\text{P3M}}$], for CAOs ranging from 1 to 7, to the expected bias $-E^{\text{cut}}_{\text{P3M}}$. The agreement is perfect for all CAOs and for all values of Ewald's splitting parameter α. The energy shift $E^{\text{cut}}_{\text{P3M}}$ in Eq. (6.6) therefore removes entirely the systematic error, as it should.

Figure 1 illustrates that the systematic errors in the uncorrected energies, which are due to cutoff and aliasing errors in the Madelung self-energies of the ions, have two different contributions of opposite sign. At small values of α, the r-space cutoff error dominates and leads to an overestimation of the energy because the negative interaction energy of an ion with the neutralizing background charge provided by the other particles is not fully taken into account. The cutoff correction (3.11) derived in Sec. III does compensate very well for this effect. At large values of α, k-space cutoff and aliasing errors dominate and lead to an underestimation of the Madelung self-energies [expression (6.4) is indeed always negative].

Since the systematic error $\langle E^{(k)}_{\text{P3M}} - E^{(k)}_{\text{exact}} \rangle$ in the reciprocal energies arise solely from self terms (the Ewald interaction between a pair of particles is zero on average), this error can alternatively, and more efficiently, be measured by computing the P3M energy of a system made up of a single ion in the box, averaging that energy over different positions of the particle relative to the mesh. To restore electroneutrality, the interaction energy (2.13) with the (implicit) neutralizing background must of course be taken into account before comparing the result with the exact Madelung self-energy $q^2\zeta/2$ of the ion. This method allows one to measure very rapidly the reciprocal contribution to the average error in the Madelung self-energies of the ions. We stress that the numerical results shown in Fig. 1 can easily be transposed to any cubic system with an arbitrary number of ions since the energy shift $E^{\text{cut}}_{\text{P3M}}$ scales merely as Q^2/L.

Having validated the energy shift (6.5), we test now the

Author complimentary copy. Redistribution subject to AIP license or copyright, see http://jcp.aip.org/jcp/copyright.jsp

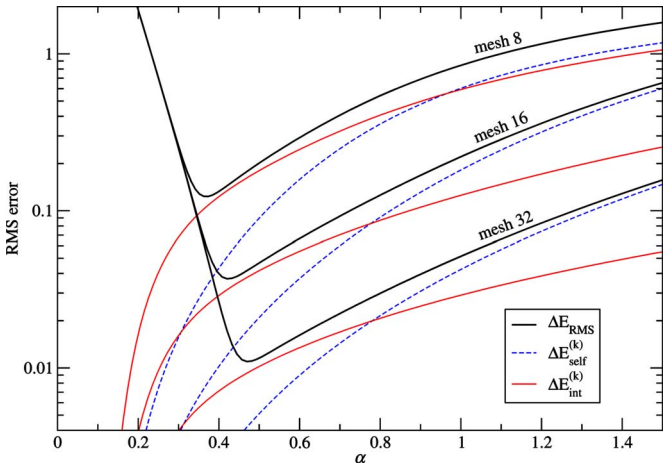

FIG. 2. (Color online) Theoretical predictions for the rms error of the corrected P3M energies for CAO 2 and three different mesh sizes (thick solid lines), for the same system and real-space cut-off as in Fig. 1. The two contributions which make up the total k-space error are also shown independently: rms error in the pair P3M interaction energies [Eq. (6.16), thin solid line] and rms error in the Madelung self-energies [Eq. (6.13), dashed line].

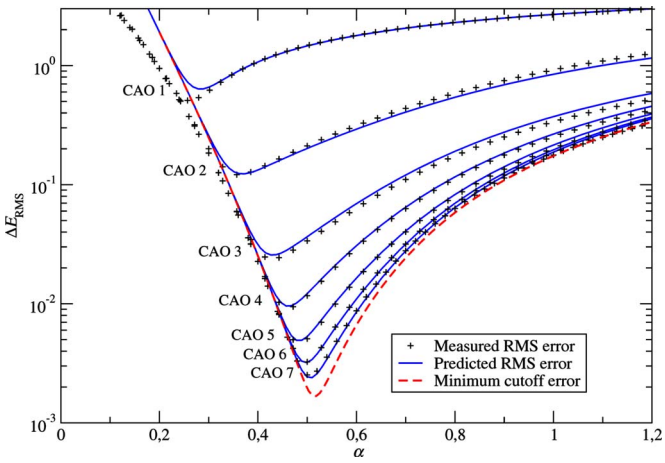

FIG. 3. (Color online) Comparison between the measured (crosses) and predicted (solid lines) rms errors of the (corrected) P3M energies, for the same test system, mesh size, and real-space cutoff as in Fig. 1. The minimal error due to direct and reciprocal space cutoffs is shown as a dashed line.

accuracy of the rms error estimate (6.19). We show in Fig. 2 the theoretical predictions for the rms error of the corrected P3M energies for different mesh sizes (thick solid lines), at fixed CAO 2. The dominant error at small values of α comes from the truncation in the real-space calculation, while k-space cutoff and aliasing errors dominate at large values of α. The plot shows also separately the contribution $\Delta E^{(k)}_{\text{self}}$, which accounts for fluctuating errors in the k-space Madelung self-energies, and the contribution $\Delta E^{(k)}_{\text{int}}$ which accounts for fluctuating errors in the P3M pair interaction energies. Near the optimal value of α, the error $\Delta E^{(k)}_{\text{int}}$ dominates slightly $\Delta E^{(k)}_{\text{self}}$ by half an order of magnitude. This validates the use of the optimal influence function (6.21), which was designed to minimize errors in the pair P3M interaction energies only. Notice that $\Delta E^{(k)}_{\text{self}}$ overcomes $\Delta E^{(k)}_{\text{int}}$ at large values of α, in agreement with the scaling with α discussed in Sec. VI. The errors in Madelung self-energies must therefore by included to predict correctly the full rms error curve in our test system with 100 charged particles, but they are expected to become negligible when the number of ions is increased above a few hundred.

The predicted rms errors agree very well with the measured rms errors, as shown in Fig. 3. The small deviations at low values of α are due to a loss of accuracy of Kolafa and Perram's r-space error estimate (2.14) and to the fact that this error estimate does not take into account the improvement in accuracy brought by the new cutoff correction term (3.11). In the regime where the dominant error comes from the k-space calculation, the agreement with our rms error estimate is excellent, especially at high values of the charge assignment order. The errors in the k-space calculation are caused by truncation and aliasing effects. The aliasing errors can be reduced by increasing the charge assignment order, but the accuracy cannot go below the minimum k-space cutoff error (6.25) (dashed curve in Fig. 3), which is intrinsic to the mesh size and choice of reciprocal interaction.

The pronounced minimum in the rms error curves stresses the importance of using the optimal value of α when performing simulations with the P3M algorithm (or with any other variant of mesh-based Ewald sums). Our accurate rms error estimate for the P3M energies can be used to quickly find the optimal set of parameters (mesh size, charge assignment order, Ewald splitting parameter) that lead to the desired accuracy with a minimum of computational effort.[29] Whatever the chosen parameters, it can serve also as a valuable indicator of the accuracy of the P3M energies.

VIII. CONCLUSIONS

In this paper, we discussed in detail which ingredients are necessary to utilize the P3M algorithm to compute accurate Coulomb energies of point charge distributions. The usage of a nearly linear scaling method ($\approx N \log N$) like P3M is almost compulsory for systems containing more than a few thousand charges.

In particular, we derived the cutoff corrections for the standard Ewald sum transparently and interpreted the systematic errors in terms of Madelung energies. This route lead us to an additional real-space cutoff correction term that has so far not been discussed in the literature. Building on these results, we have deduced the k-space cutoff correction term in the case of the P3M algorithm, where additional aliasing errors play a role. Furthermore, we derived the exact form of the influence function that minimizes the rms errors in the energies, and showed that this function is not much different from the force-optimized influence function, which *a posteriori* justifies why in most P3M implementations the usage of the force-optimized influence function does not lead to inaccurate results. Based on the energy optimized influence function we derive an accurate rms error estimate for the energy and performed numerical tests on sample configurations that demonstrate the validity of our error estimates and the necessity to include our correction terms. We also demonstrated that the electrostatic energy of an individual particle in the system can be obtained in the P3M method, but at the expense of an additional inverse fast Fourier transform.

Author complimentary copy. Redistribution subject to AIP license or copyright, see http://jcp.aip.org/jcp/copyright.jsp

With the help of the newly derived error estimates we can easily tune the desired accuracy of the P3M algorithm and find suitable parameter combinations before running any simulation.

The P3M algorithm can be generalized along our discussed lines to compute other long range interactions. Of particular interest are dipolar energies, forces and torques, and the associated error estimates for these quantities. This will be the content of a forthcoming publication. Our P3M generalization for the energies will be included in a future version of the molecular simulation package ESPRESSO,[30] that is freely available under the GNU general public license. (For up-to-date information, see Ref. 31.)

ACKNOWLEDGMENTS

Funds for this research were provided by the Volkswagen Stiftung under Grant No. I/80433 and by the DFG within Grant No. Ho-1108/13-1.

APPENDIX A: EWALD PAIR POTENTIAL AND MADELUNG SELF-ENERGY

The Ewald formula for the electrostatic energy E of a periodic charged system can be written in a form that underlines the fact that E includes the Madelung self-energies $Q^2\zeta/2$ of the ions [$Q^2=\Sigma_i q_i^2$ and ζ is defined in Eq. (3.7)]. We recall from Sec. II that the Ewald formula for E reads, if the system is globally neutral and if we employ metallic boundary conditions

$$E=\frac{1}{2}\sum_{i,j}{}'\sum_{\boldsymbol{n}\in\mathbb{Z}^3} q_i q_j \psi(\boldsymbol{r}_{ij}+\boldsymbol{n}L) + \frac{1}{2L^3}\sum_{i,j} q_i q_j \sum_{\substack{\boldsymbol{k}\in\mathbb{K}\\ \boldsymbol{k}\neq 0}} e^{-i\boldsymbol{k}\cdot(\boldsymbol{r}_i-\boldsymbol{r}_j)}\tilde{\phi}(\boldsymbol{k}) - Q^2\frac{\alpha}{\sqrt{\pi}}. \tag{A1}$$

The "self-energy terms" in E, i.e., term $E^{(s)}$ and terms $i=j$, are

$$\frac{Q^2}{2}\left(\sum_{\boldsymbol{n}\neq 0}\psi(\boldsymbol{n}L)+\frac{1}{L^3}\sum_{\boldsymbol{k}\neq 0}\tilde{\phi}(\boldsymbol{k})-\frac{2\alpha}{\sqrt{\pi}}\right)=\frac{Q^2}{2}\left(\zeta+\frac{\pi}{\alpha^2L^3}\right). \tag{A2}$$

We can therefore write

$$E=\frac{1}{2}\sum_{i\neq j} q_i q_j\left(\sum_{\boldsymbol{n}\neq 0}\psi(\boldsymbol{r}_{ij}+\boldsymbol{n}L)+\frac{1}{L^3}\sum_{\boldsymbol{k}\neq 0} e^{-i\boldsymbol{k}\cdot\boldsymbol{r}_{ij}}\tilde{\phi}(\boldsymbol{k})\right) + \frac{Q^2}{2}\left(\zeta+\frac{\pi}{\alpha^2L^3}\right)=\frac{1}{2}\sum_{i\neq j} q_i q_j V_{\mathrm{Ewald}}(\boldsymbol{r}_{ij})+\frac{Q^2}{2}\zeta, \tag{A3}$$

where we defined the Ewald pair interaction[11]

$$V_{\mathrm{Ewald}}(\boldsymbol{r})=\sum_{\boldsymbol{n}\neq 0}\psi(\boldsymbol{r}+\boldsymbol{n}L)+\frac{1}{L^3}\sum_{\boldsymbol{k}\neq 0} e^{-i\boldsymbol{k}\cdot\boldsymbol{r}}\tilde{\phi}(\boldsymbol{k})-\frac{\pi}{\alpha^2L^3}. \tag{A4}$$

Notice that in writing Eq. (A3), we used $\Sigma_i\Sigma_{j\neq i} q_i q_j \pi/(\alpha^2L^3)=-Q^2\pi/(\alpha^2L^3)$ which follows from electroneutrality. Thanks to the inclusion of this constant in the definition of $V_{\mathrm{Ewald}}(\boldsymbol{r})$, the Ewald pair potential does not depend on the parameter α [$\partial/\partial\alpha V_{\mathrm{Ewald}}(\boldsymbol{r})=0$] and its average over the simulation box is zero[32]

$$\langle V_{\mathrm{Ewald}}(\boldsymbol{r})\rangle=\frac{1}{L^3}\int_{L^3} \mathrm{d}^3\boldsymbol{r}\, V_{\mathrm{Ewald}}(\boldsymbol{r})=0. \tag{A5}$$

The latter property is simply a consequence of $\langle\exp(i\boldsymbol{k}\cdot\boldsymbol{r}_{ij})\rangle=\delta_{\boldsymbol{k},0}$ and Eq. (3.5).

In conclusion, expression (A3) shows explicitly that the electrostatic energy of a periodic charged system includes the Madelung self-energies $Q^2\zeta/2$ of the ions.[22,23] The fact that the Ewald interaction between a pair of particles averages to zero when one particle explores the whole simulation box is also noteworthy aspect of Ewald potential.[32]

APPENDIX B: PROOF OF Eq. (5.2)

Equation (5.2) is a consequence of the sampling theorem and is straightforward to demonstrate. The sum in Eq. (4.3) is rewritten as an integral

$$\tilde{\rho}_{\mathrm{M}}(\boldsymbol{k})=h^3\int \mathrm{d}\boldsymbol{r}'\int_V \mathrm{d}\boldsymbol{r}\,\mathrm{III}(\boldsymbol{r})U(\boldsymbol{r}-\boldsymbol{r}')\rho(\boldsymbol{r}')e^{-i\boldsymbol{k}\cdot\boldsymbol{r}}, \tag{B1}$$

where we used Eq. (4.1) and introduced an infinite mesh of Dirac delta functions

$$\mathrm{III}(\boldsymbol{r})=\sum_{\boldsymbol{r}_m\in\mathbb{M}_p}\delta(\boldsymbol{r}-\boldsymbol{r}_m)=\frac{1}{h^3}\sum_{\boldsymbol{m}\in\mathbb{Z}^3} e^{-ik_g\boldsymbol{m}\cdot\boldsymbol{r}}. \tag{B2}$$

(We recall that $k_g=2\pi/h$). Using the earlier representation of III($\boldsymbol{r}$) and introducing in Eq. (B1) the Fourier series representation of the periodic charge density,

$$\rho(\boldsymbol{r}')=\frac{1}{L^3}\sum_{\boldsymbol{k}'\in\mathbb{K}}\tilde{\rho}(\boldsymbol{k}')\exp(i\boldsymbol{k}'\cdot\boldsymbol{r}'), \tag{B3}$$

we recover the result (5.2) after straightforward simplifications.

APPENDIX C: PROOF OF EQUIVALENCE BETWEEN Eqs. (4.9) and (4.6)

Equation (4.9) is equivalent to

$$E_{\mathrm{P3M}}^{(ks)}=\frac{1}{2V}\sum_{\substack{\boldsymbol{k}\in\mathbb{K}\\ \boldsymbol{k}\neq 0}}\tilde{\rho}^*(\boldsymbol{k})\tilde{\Phi}(\boldsymbol{k}), \tag{C1}$$

where $\tilde{\Phi}(\boldsymbol{k})$ is the full Fourier transform ($\boldsymbol{k}\in\mathbb{K}$) of the back-interpolated potential mesh (4.8),

$$\tilde{\Phi}(\boldsymbol{k})=\int_V\Phi(\boldsymbol{r})\mathrm{d}\boldsymbol{r}=h^3\int_V\mathrm{d}\boldsymbol{r}e^{-i\boldsymbol{k}\cdot\boldsymbol{r}}\int\mathrm{d}\boldsymbol{r}'\,\mathrm{III}(\boldsymbol{r}')U(\boldsymbol{r}-\boldsymbol{r}')\times\Phi_{\mathrm{M}}(\boldsymbol{r}'). \tag{C2}$$

We replace in this equation $\Phi_{\mathrm{M}}(\boldsymbol{r}')$ and III($\boldsymbol{r}'$) by their expressions (4.7) and (C2) and perform the integration over $\boldsymbol{r}'$,

Author complimentary copy. Redistribution subject to AIP license or copyright, see http://jcp.aip.org/jcp/copyright.jsp

$$\tilde{\Phi}(\boldsymbol{k}) = \frac{1}{L^3} \sum_{\boldsymbol{k}' \in \tilde{\mathbb{M}}} \tilde{\Phi}_{\mathrm{M}}(\boldsymbol{k}') \sum_{\boldsymbol{m}} \int_V \mathrm{d}\boldsymbol{r} e^{-i\boldsymbol{k}\cdot\boldsymbol{r}} \tilde{U}(\boldsymbol{k}' + k_g \boldsymbol{m}) e^{i(\boldsymbol{k}' + k_g \boldsymbol{m})\cdot\boldsymbol{r}}. \tag{C3}$$

The integration over $\boldsymbol{r}$ introduces a Kronecker symbol $\delta_{\boldsymbol{k},\boldsymbol{k}'+k_g\boldsymbol{m}}$. We therefore get the simple result

$$\tilde{\Phi}(\boldsymbol{k}) = \tilde{\Phi}_{\mathrm{M}}(\boldsymbol{k}) \tilde{U}(\boldsymbol{k}), \tag{C4}$$

where the function $\tilde{\Phi}_{\mathrm{M}}(\boldsymbol{k})$, which is defined originally only for $\boldsymbol{k} \in \tilde{\mathbb{M}}$, is now understood to be extended periodically to all $\mathbb{K}$ space. Notice that the inverse FFT does not introduce aliasing errors: the sum over $\boldsymbol{m}$ merely renders $\tilde{\Phi}_{\mathrm{M}}(\boldsymbol{k})$ periodic. In accordance with Eqs. (4.3) and (4.5), we extend also $\tilde{\rho}_{\mathrm{M}}(\boldsymbol{k})$ and $\tilde{G}(\boldsymbol{k})$ periodically, with period $2\pi/h$. Using the earlier result and Eq. (4.5), the reciprocal energy (C1) can be expressed as

$$\begin{aligned} E_{\mathrm{P3M}}^{(ks)} &= \frac{1}{2L^3} \sum_{\boldsymbol{k} \in \mathbb{K}} \tilde{\rho}^*(\boldsymbol{k}) \tilde{U}(\boldsymbol{k}) \tilde{\rho}_{\mathrm{M}}(\boldsymbol{k}) \tilde{G}(\boldsymbol{k}) \\ &= \frac{1}{2L^3} \sum_{\boldsymbol{k} \in \tilde{\mathbb{M}}} \sum_{\boldsymbol{m} \in \mathbb{Z}^3} \tilde{\rho}^*(\boldsymbol{k} + k_g \boldsymbol{m}) \tilde{U}(\boldsymbol{k} + k_g \boldsymbol{m}) \tilde{\rho}_{\mathrm{M}}(\boldsymbol{k}) \tilde{G}(\boldsymbol{k}). \end{aligned} \tag{C5}$$

This may be compared with Eq. (4.6), i.e.,

$$E_{\mathrm{P3M}}^{(ks)} = \frac{1}{2L^3} \sum_{\substack{\boldsymbol{k} \in \tilde{\mathbb{M}} \\ \boldsymbol{k} \neq 0}} \tilde{\rho}_M^*(\boldsymbol{k}) \tilde{\rho}_M(\boldsymbol{k}) \tilde{G}(\boldsymbol{k}). \tag{C6}$$

Recalling Eq. (5.2) and the fact that $\tilde{U}(\boldsymbol{k})$ is real, we see that both expressions are equivalent.

[1] S. Sagui and T. A. Darden, Annu. Rev. Biophys. Biomol. Struct. **28**, 155 (1999).
[2] A. Arnold and C. Holm, *Advanced Computer Simulation Approaches for Soft Matter Sciences II*, Series: Adv. Polym. Sci. 185 (Springer, Berlin, 2005), pp. 59–109.
[3] R. W. Hockney, S. P. Goel, and J. W. Eastwood, Chem. Phys. Lett. **21**, 589 (1973).
[4] R. W. Hockney and J. W. Eastwood, *Computer Simulation Using Particles* (IOP, Bristol, 1988).
[5] J. W. Eastwood, R. W. Hockney, and D. N. Lawrence, Comput. Phys. Commun. **19**, 215 (1980).
[6] T. Darden, D. York, and L. G. Pedersen, J. Chem. Phys. **98**, 10089 (1993).
[7] U. Essmann, L. Perera, M. L. Berkowitz, T. Darden, H. Lee, and L. G. Pedersen, J. Chem. Phys. **103**, 8577 (1995).
[8] T. A. Darden, A. Toukmaji, and L. G. Pedersen, J. Chim. Phys. **94**, 1346 (1997).
[9] M. Deserno and C. Holm, J. Chem. Phys. **109**, 7678 (1998).
[10] C. Sagui and T. A. Darden, in *Simulation and Theory of Electrostatic Interactions in Solution*, edited by L. R. Pratt and G. Hummer (AIP, Melville, NY, 1999), pp. 104–113.
[11] S. W. de Leeuw, J. W. Perram, and E. R. Smith, Proc. R. Soc. London, Ser. A **373**, 57 (1980).
[12] J.-M. Caillol, J. Chem. Phys. **101**, 6080 (1994).
[13] E. R. Smith, Mol. Phys. **65**, 1089 (1988).
[14] V. Ballenegger and J.-P. Hansen, J. Chem. Phys. **122**, 114711 (2005).
[15] J. Kirkwood, J. Chem. Phys. **7**, 911 (1939).
[16] A. Alastuey and V. Ballenegger, Physica A **279**, 268 (2000).
[17] V. Ballenegger and J.-P. Hansen, Mol. Phys. **102**, 599 (2004).
[18] P. Ewald, Ann. Phys. **369**, 253 (1921).
[19] G. Hummer, L. R. Pratt, and A. E. García, J. Phys. Chem. **99**, 14188 (1995).
[20] M. P. Allen and D. J. Tildesley, *Computer Simulation of Liquids, Oxford Science Publications* (Clarendon, Oxford, 1987).
[21] J. Kolafa and J. W. Perram, Mol. Simul. **9**, 351 (1992).
[22] S. G. Brush, H. L. Sahlin, and E. Teller, J. Chem. Phys. **45**, 2102 (1966).
[23] B. R. Nijboer and T. W. Ruijgrok, J. Stat. Phys. **53**, 361 (1988).
[24] T. Darden, D. Pearlman, and L. G. Pedersen, J. Chem. Phys. **109**, 10921 (1998).
[25] Z. Wang and C. Holm, J. Chem. Phys. **115**, 6351 (2001).
[26] J. W. Eastwood, in *Computational Methods in Classical and Quantum Physics*, edited by D. J. Evans and S. Chomet (Advance Publications, Ltd., London, 1976), pp. 206–228.
[27] E. L. Pollock and J. Glosli, Comput. Phys. Commun. **95**, 93 (1996).
[28] B. A. Luty, I. G. Tironi, and W. F. van Gunsteren, J. Chem. Phys. **103**, 3014 (1995).
[29] M. Deserno and C. Holm, J. Chem. Phys. **109**, 7694 (1998).
[30] H. J. Limbach, A. Arnold, B. A. Mann, and C. Holm, Comput. Phys. Commun. **174**, 704 (2006).
[31] The website http://www.espresso.mpg.de provides up-to-date information.
[32] G. Hummer, L. R. Pratt, and A. E. García, J. Phys. Chem. A **102**, 7885 (1998).

Author complimentary copy. Redistribution subject to AIP license or copyright, see http://jcp.aip.org/jcp/copyright.jsp